Cement and Concrete Composites 114 (2020) 103772

Contents lists available at ScienceDirect

Cement and Concrete Composites

journal homepage: http://www.elsevier.com/locate/cemconcomp

Performance of lime-metakaolin pastes using gravel wash mud (GWM)

Vishojit Bahadur Thapa, Danièle Waldmann *

Laboratory of Solid Structures, University of Luxembourg, L-4364, Esch-sur-Alzette, Luxembourg

ARTICLE INFO

Keywords:
Gravel wash mud
Lime
Metakaolin
Calcined clays
Mineralogy
Mechanical properties
Pozzolanic activity

ABSTRACT

The performance of ternary binders using lime, metakaolin (MK) and gravel wash mud (GWM) powders is studied for the development of novel lime-pozzolan pastes. This study examines the influence of varying mixture proportions using different types and compositions of lime powders and GWM at different treatment levels on the mechanical properties of lime-MK-GWM pastes. Various characterisation techniques including particle size distribution (PSD), X-ray fluorescence (XRF), X-ray diffraction (XRD), compressive strength tests, simultaneous thermal analysis (STA) and scanning electron microscopy (SEM), were applied on the different raw materials, respectively, on the hardened pastes to determine the reaction kinetics, the resulting microstructure and the mechanical performances of the lime-MK-GWM binder systems. Higher strength-enhancing contributions of thermally treated GWM powders (calcined at 850 °C) leading to compressive strengths up to 18 MPa were confirmed and the strength-based evaluations revealed that hydrated lime-based pastes achieved higher mechanical performances than hydraulic lime-based binder systems.

1. Introduction

Combating climate change has undoubtedly become one of the major global priority concerns and its success crucially depends on the reduction of CO_2 emissions related to the cement industry, more precisely the cement clinker production [1–4]. In modern cement kilns, the production of 1 tonne of cement clinker generates around 800–840 kg gross CO_2 emissions [1,5], out of which about two third of the CO_2 emissions are released during the calcination reaction (decarbonation of calcium carbonate $CaCO_3$ into lime CaO and CO_2) and one third results from the combustion process itself [3,4]. Moreover, for further reduction of the overall carbon footprint of ordinary Portland cement (OPC), it is current practice for cement manufacturers to complement the Portland clinker by various cementitious products as partial clinker replacement materials or as additions, which are mainly reactive alumina-siliceous industrial co-products and are deemed to be low carbon in compliance with the cement standards [6]. In recent decades, extensive research was carried out to develop environmental friendly and sustainable binder technologies allowing to reduce the usage of cement clinker by using industrial by-products or waste materials, instead of already established and commercially available cement additions like fly ash (FA), ground granulated blast furnace slag (GGBS) and silica fume (SF) [7–12]. Especially in Europe, with the decline of the primary industrial activities in coal power stations, the steel industry and the ferro-alloy and silicon production, the availability of these resources has gradually dried up and remaining activities are no longer found sufficiently close to the cement production sites.

Most of the research studies investigate on supplementary cementitious materials (SCMs) and on how the clinker contents in Portland cement can be reduced without loss in workability, performance and durability. In particular, investigations on alternative SCMs using naturally occurring raw clays mixes and waste clay products have risen worldwide [13–19]. Among recently investigated aluminosilicate materials figure the gravel wash mud (GWM) powders [14] and the sewage sludge ashes [19], which originally are waste products of industrial activities (sandstone quarry and sludge incineration plants). Their strength-enhancing potentials as promising alternative SCM in cement-based pastes, respectively in lime-pozzolan systems, were confirmed.

Furthermore, recent trends promote research on lime-based binder concepts without Portland cement clinker to develop mortars and concrete products using alternative cementitious materials like ground granulated blast-furnace slag, pulverised fuel ash, calcined clays, silica fume, rice husk ash, and brick dusts [11,20–22]. From a historical aspect, lime-pozzolan binders are the predecessor binder systems of Portland cement clinker and lime-pozzolan plasters have gained greater interest as valuable alternatives to OPC-based mortars for the restoration of historical buildings due to their better compatibility with historic

* Corresponding author.
E-mail address: daniele.waldmann@uni.lu (D. Waldmann).

https://doi.org/10.1016/j.cemconcomp.2020.103772
Received 7 July 2020; Received in revised form 30 July 2020; Accepted 3 August 2020
Available online 19 August 2020

lime-based building structures [23–28]. However, the increasing political and societal awareness on reducing the immediate impacts of climate change have imposed operational restrictions on intense CO_2-emitting industrial sectors like the cement industry. Therefore, in the recent years, the investigations on lime-pozzolan binders have significantly risen up [19,25,29–36]. In general, the hardening mechanism of pure lime binders is mainly driven by carbonation reaction, a slow reaction process where calcium hydroxide reacts with atmospheric CO_2 to form calcium carbonates [37,38]. However, in the presence of reactive, aluminosilicate-rich pozzolanic materials, the hydration reaction is favoured with formation of hydraulic components. The reaction mechanisms of binary lime-metakaolin binders systems were investigated in Ref. [21–23,32,35] and they confirmed that the main initial phases formed are (cementitious) hydraulic products like calcium silicate hydrates (CSH), calcium aluminate silicate hydrates (CAH) and calcium aluminate silicate hydrates (CASH) resulting from the pozzolanic reaction between the calcium hydroxide-rich limes and the pozzolans. The compositional variety, the stability and the durability of these compounds depends on the amorphous phases in the alumina-siliceous materials, which strongly influence its pozzolanicity as well as the resulting mechanical performances [11]. Mechanical performances up to 28 MPa were reported in Ref. [25,36] for binary lime-silica fume pastes, ternary lime-silica fume-GGBS pastes and lime-fly ash-ceramic waste pastes; as well as compressive strength around 14 MPa for lime-MK pastes in combination with other pozzolanic additions. Furthermore, valuable research has been made into understanding the long-term characteristics of the corresponding lime-MK pastes [31,39]. Both studies concluded that with increasing curing age, the stability of the formed hydraulic compounds depends on the optimal MK content in correlation with consumable calcium hydroxide content to restrict the early carbonation reaction and promote later carbonate hardening.

However, most of the works focus mainly on the reaction kinetics of lime-MK systems for heritage restoration purposes, therefore, little is known about the impacts on the reaction mechanisms, the mechanical performances, the durability, the optimal composition (hydraulic or hydrated lime) and the performance-enhancing characteristics of lime-MK binders using alternative SCMs [19,34,40].

This paper focuses its investigations on the strength-enhancing pozzolanic character of gravel wash mud (GWM) as SCM in ternary lime-MK-GWM binder systems. GWM, a quarry waste product, was incorporated in lime-MK pastes using varying raw material compositions and different mix designs. The primary aim is to determine the optimal prime material compositions and to investigate towards optimal mix proportions by conducting a selected set of physiochemical and mineralogical characterisation analyses and performance-based experimental assessments on the lime-MK-GWM products. Large series of lime-MK-GWM pastes were prepared including GWM in three different states of matter (pure, uncalcined and calcined at 850 °C [13,14]), hydraulic lime, three different hydrated limes, MK and fine dolomitic sand. The physiochemical and mineralogical characterisations of selected raw materials were determined using laser diffraction granulometry, the X-ray fluorescence (XRF) analysis, the quantitative X-ray diffraction (XRD) analysis and the simultaneous thermal analysis (STA). The actual potential of ternary lime-MK-GWM pastes was drawn out based on the evaluation of hardened samples using mechanical strength tests combined with thermal analysis and scanning electron microscopy.

2. Materials and experimental program

2.1. Materials and material preparations

Three different hydrated limes, HL1 ($\rho_{HL1} = 0.55$ g/cm^3) from Lhoist (Istein, Germany), HL2 ($\rho_{HL2} = 0.52$ g/cm^3) and HL3 ($\rho_{HL3} = 0.41$ g/cm^3) from Carmeuse S.A. (Belgium), were selected for this study to investigate the required characteristics of hydrated limes for optimal use. HL1 and HL3 are classified as calcium limes CL90-S (CaO + MgO content $\geq$ 90 wt%; S stands for powder) and HL2 as CL80-S (CaO + MgO content $\geq$ 80 wt%; S stands for powder), according to EN 459–1:2010 [41]. For the comparative trial test, a natural hydraulic lime (NHL, $\rho_{NHL} = 0.65$ g/cm^3) from Chaux et enduits de Saint-Astier (France), classified as natural hydraulic lime NHL 3.5 ($Ca(OH)_2$ content $\geq$ 25 wt%, 28-day compressive strength $\geq$ 3.5 MPa to $\leq$ 10 MPa) according to Ref. [41] was used.

The used metakaolin (MK, $\rho_{MK} = 0.87$ g/cm^3) is produced by Argeco Développement (France) according to NF P18-513 [42] by milling and calcining the raw kaolinite using the flash calcination method. In addition, a fine dolomitic sand (DS, $\rho_{DS} = 1.71$ g/cm^3) from Carrières Feidt S.A. (Luxembourg) was used as fine aggregate.

Pure gravel wash mud (PGWM) was sampled from a decantation basin from a local sandstone quarry operated by Carrières Feidt S.A. (Luxembourg). The wet GWM has a water content of around 32 wt% (with use of a flocculation reagent) [13]. After removal of the absorbed water and moisture by drying the sludge at 105 °C in a laboratory drying chamber for two days, the dried GWM was fragmented and ground into a fine powder, denominated as uncalcined GWM (UGWM, $\rho_{UGWM} = 0.75$ g/cm^3) powder. The calcination of the UGWM powder into a more reactive, amorphous raw material, henceforth referred to as calcined GWM (CGWM, $\rho_{CGWM} = 0.73$ g/cm^3) powder, was performed in a laboratory chamber furnace with radiation heating by burning the fine powders from room temperature up to 850 °C (heating rate of 5 °C/min) [14]. After application of the peak temperature for 1 h, the CGWM powder is let to cool down naturally inside the chamber furnace.

This study examines the suitability of the proposed MK-lime-GWM pastes as a potential alternative to OPC-based products for constructive applications. Prior to the investigated mixtures, preliminary strength-based evaluations were carried out to restrict the study range of the examined mixture proportions. Within this work, over 250 specimens were prepared based on varying mixing proportions of different types and compositions of lime powders (NHL, HL1, HL2 and HL3), GWM in different forms and treatment levels (PGWM, UGWM and CGWM), commercial Metakaolin (MK) and dolomitic sand (DS) as fine aggregate. The initial focus was on the selection of the adequate raw materials (types of lime and GWM) with the objective to restrict the range of examined mixture proportions towards optimum and the evaluation of the reaction mechanisms to achieve best possible performances of the investigated binder concepts.

2.2. Paste compositions, mix proportion design and curing conditions

The mix design (Table 1) comprises three series of mixtures, which were adapted and prepared consecutively based on the findings of the respective preceding series. Three specimens of each mixture were prepared for each investigated curing age. The first series of mixtures (S1; curing ages of 7, 14, 28 days) consists of pastes based on pure, untreated GWM (PGWM), MK, and DS with two types of limes, namely natural hydraulic lime (NHL) or hydrated calcium lime (HL1). This primary set of mixtures examines the potential of binders using pure GWM as a potential raw material before any treatment procedures of this raw product are adopted which would lead to modifications of the mineralogy and the microstructure. In addition, a reliable statement on the choice of lime type (hydraulic or hydrated lime) as well as the range of acceptable mixture proportions was developed. Including additional mixture adjustments by taking into account the findings of the first series, the second series of mixtures (S2; curing ages of 7, 14, 28 and 90 days) examines pastes based on PGWM, MK and DS with three different hydrated limes HL1, HL2 and HL3, to evaluate the optimal physiochemical characteristics and compositions of hydrated limes using strength-based performance criteria. Based on the results of the second series of mixtures, the third and largest series of mixtures (S3; curing ages of 7, 28, 56 and 90 days) consists of pastes based on HL2, MK, DS and processed GWM powder (UGWM or CGWM), and a control lime-MK

Table 1
Mix proportions of studied mix series.

Series 1 (S1)	Mix proportions by mass					
	NHL	HL1	MK	PGWM	w/b[a]	ag/b[b]
	[−]	[−]	[−]	[−]	[−]	[−]
PGA_NHL	1.00	–	2.00	1.00	0.30	0.70
PGB_NHL	1.00	–	1.66	1.25	0.30	0.70
PGC_NHL	1.00	–	0.70	1.40	0.30	0.70
PGA_HL1	–	1.00	2.00	1.00	0.30	0.70
PGB_HL1	–	1.00	1.66	1.25	0.30	0.70
PGC_HL1	–	1.00	0.70	1.40	0.30	0.70

Series 2 (S2)	**Mix proportions by mass**						
	HL1	HL2	HL3	MK	PGWM	w/b[a]	ag/b[b]
	[−]	[−]	[−]	[−]	[−]	[−]	[−]
PG_HL1	1.00	–	–	1.33	1.00	0.45	0.70
PG_HL2	–	1.00	–	1.33	1.00	0.45	0.70
PG_HL3	–	–	1.00	1.33	1.00	0.45	0.70

Series 3 (S3)	**Mix proportions by mass**					
	HL2	MK	UGWM	CGWM	w/b[a]	ag/b[b]
	[−]	[−]	[−]	[−]	[−]	[−]
REF	1.00	1.33	–	–	0.50	0.70
UG_1:1:1	1.00	1.00	1.00	–	0.50	0.70
UG_1:1:1.33	1.00	1.00	1.33	–	0.50	0.70
UG_1:1:1.66	1.00	1.00	1.66	–	0.50	0.70
UG_1:1.33:1	1.00	1.33	1.00	–	0.50	0.70
UG_1:1.33:1.33	1.00	1.33	1.33	–	0.50	0.70
UG_1:1.33:1.66	1.00	1.33	1.66	–	0.50	0.70
UG_1:1.66:1	1.00	1.66	1.00	–	0.50	0.70
UG_1:1.66:1.33	1.00	1.66	1.33	–	0.50	0.70
UG_1:1.66:1.66	1.00	1.66	1.66	–	0.50	0.70
CG_1:1:1	1.00	1.00	–	1.00	0.50	0.70
CG_1:1:1.33	1.00	1.00	–	1.33	0.50	0.70
CG_1:1:1.66	1.00	1.00	–	1.66	0.50	0.70
CG_1:1.33:1	1.00	1.33	–	1.00	0.50	0.70
CG_1:1.33:1.33	1.00	1.33	–	1.33	0.50	0.70
CG_1:1.33:1.66	1.00	1.33	–	1.66	0.50	0.70
CG_1:1.66:1	1.00	1.66	–	1.00	0.50	0.70
CG_1:1.66:1.33	1.00	1.66	–	1.33	0.50	0.70
CG_1:1.66:1.66	1.00	1.66	–	1.66	0.50	0.70

[a] w/b: water/binder ratio, binder equal to mass of lime, MK and GWM.
[b] ag/b: binder/aggregate ratio; ag: dolomitic sand (DS).

paste mixture without GWM content (REF). These series lead to the reported maximum performances of the proposed binder concepts with adapted mix design proportions. The water/binder (w/b) ratio was adjusted from one series to another from 0.3 to 0.5 and the aggregate/binder (ag/b) ratio was kept constant at 0.7.

The mixing procedure was the same for all the series of mixtures: the amounts of binder components, namely GWM, MK, and lime, were dry-mixed at a mixing speed of 125 rpm for 15s. While maintaining the same mixing speed, half of the water is gradually added and let to mix for another 180s. Subsequently, the amount of DS is added with the remaining water and the compound is mixed for 90 s at 125 rpm and finally 90 s at 250 rpm. The fresh mixture pastes were cast in prismatic moulds (40 × 40 × 160 mm^3) and compacted for 15 s on a vibrating table. After casting, the moulds were covered with plastic plates of 5 mm thickness to prevent rapid desiccation. After hardening time of 24 h, the specimens were demoulded, wrapped in cellophane foil to restrict moisture exchange with the surroundings and cured at ambient temperature until 24 h before the uniaxial compression tests according to EN 196–1 [43].

2.3. Experimental methods

The particle size distributions of NHL, HL1, HL2, HL3, UGWM, CGWM, DS and MK powders were determined by the laser diffraction technique using a particle size analyser (HELOS-RODOS-VIBRI from Sympatec GmbH, Germany). The chemical composition of the powder samples was determined by X-ray fluorescence method using a wavelength dispersive X-ray fluorescence spectrometer (S8 TIGER from Bruker AXS GmbH, Germany).

A powder X-ray diffractometer (D4 ENDEAVOR from Bruker AXS GmbH) using Cu K_α radiation was used to determine the mineralogy of the powders by quantitative X-ray diffraction analysis, following the Rietveld refinement principles. The characteristic d-spacings and diffraction peak intensities corresponding to specific crystalline phases, available in the powder samples, were detected using the XRD software DIFFRAC.EVA (Bruker AXS GmbH, Germany). The XRD patterns were processed using the software TOPAS (Bruker Corporation) using the fundamental parameter approach for line profile fitting [44]. Moreover, the crystalline phases were described using appropriate structural data from ICSD database [14,45,46] before refinement of the diffractograms using the Rietveld method [47,48]. The amorphous contents were computed using quartz at 35% as an internal reference as described in Ref. [14,46].

The thermo-analytical technique applied on the hardened binder pastes was the simultaneous thermal analysis (STA), which merges the techniques to monitor the heat flow change (differential scanning calorimetry, DSC) and the mass change (thermogravimetric analysis, TGA) of a sample as a function of temperature.

The compressive strength of each mixture was measured on three replicate specimens for each curing age. The strength assessment was carried out using a compression test plant (TONICOMP III, Toni Technik GmbH, Germany), conform to the standard DIN EN 196–1 [43], with additional displacement transducers.

The microstructural composition of the hardened specimens were examined by scanning electron microscopy (SEM) using a "LEO 440 REM" unit (Carl Zeiss SMT AG, Germany). The examined samples were small fractions from the compressed specimens, which were prepared for the SEM analysis by applying a functional gold coating on the non-conductive.

3. Results and discussions

3.1. Physicochemical properties of the primary materials

Table 2 shows the chemical analysis of the used primary materials for the paste compositions. The different types of hydrated limes (HL1, HL2 and HL3) confirm a major CaO content, mainly resulting from the portlandite minerals. The natural hydraulic lime (NHL) shows a slightly lower CaO content and a medium silica (SiO_2) content, resulting from the presence of argillaceous components during the firing process to produce calcium silicate compounds. The GWM powders (UGWM and CGWM) and the Metakaolin (MK) can be categorised as aluminosilicate-rich materials with high silica (SiO_2) and medium alumina (Al_2O_3) contents [13,14]. However, UGWM and CGWM show a slightly lower alumina (Al_2O_3) content, but higher ferrite (Fe_2O_3) content than MK, which explains the comparatively darker brownish-red colour of the GWM powders. The dolomitic sand (DS) shows high CaO, medium SiO_2 and MgO contents, which can be assigned to the high presence of calcium-magnesium carbonate phases (dolomite).

The particle size distributions of the used materials are displayed in Fig. 1. The different primary materials show a very fine PSD ranging from a fine clay particle size (<2 μm) up to a coarse silt grain size (<60 μm). Among the investigated materials, the three hydrated limes show the finest grain size range (d10-d90) from 0.7 to 5.5 μm with respective mean particle sizes (d50) and high specific surface areas of 2.23 μm and 1169.9 m^2/kg for HL1, 1.41 μm and 1597.2 m^2/kg for HL2, and respectively,1.45 μm and 1554.3 m^2/kg for HL3. In comparison, NHL presents a higher average particle size of 7.54 μm and a lower specific surface area of 628.3 m^2/kg. The UGWM and CGWM powders follow very similar PSD with d50 of 7.36 μm resp. 8.36 μm and specific surface areas of 522.5 m^2/kg resp. 479.9 m^2/kg. CGWM is slightly coarser than

Table 2
Chemical composition of applied materials: HL1, HL2, HL3, UGWM, CGWM (calcined at 850 °C), DS and MK powders.

Sample	Chemical composition									
	SiO_2	Al_2O_3	Fe_2O_3	CaO	MgO	SO_3	Na_2O	K_2O	TiO_2	MnO
[–]	[%]	[%]	[%]	[%]	[%]	[%]	[%]	[%]	[%]	[%]
HL1	0.57	0.50	0.28	96.86	0.95	0.26	0.17	–	–	–
HL2	0.14	0.14	0.07	98.62	0.50	0.11	0.15	–	–	–
HL3	–	–	0.07	98.78	0.53	0.10	–	–	–	–
NHL	18.35	2.13	0.86	75.63	1.54	0.68	0.11	0.39	0.10	0.02
UGWM	64.97	19.50	9.35	0.41	1.66	0.09	0.24	2.72	0.85	0.06
CGWM	64.01	20.26	8.90	0.41	1.81	–	0.24	3.25	0.90	0.08
DS	22.54	4.79	5.16	49.25	13.91	0.18	–	2.54	0.57	0.20
MK	69.37	32.01	2.74	0.99	–	–	–	0.31	1.41	–

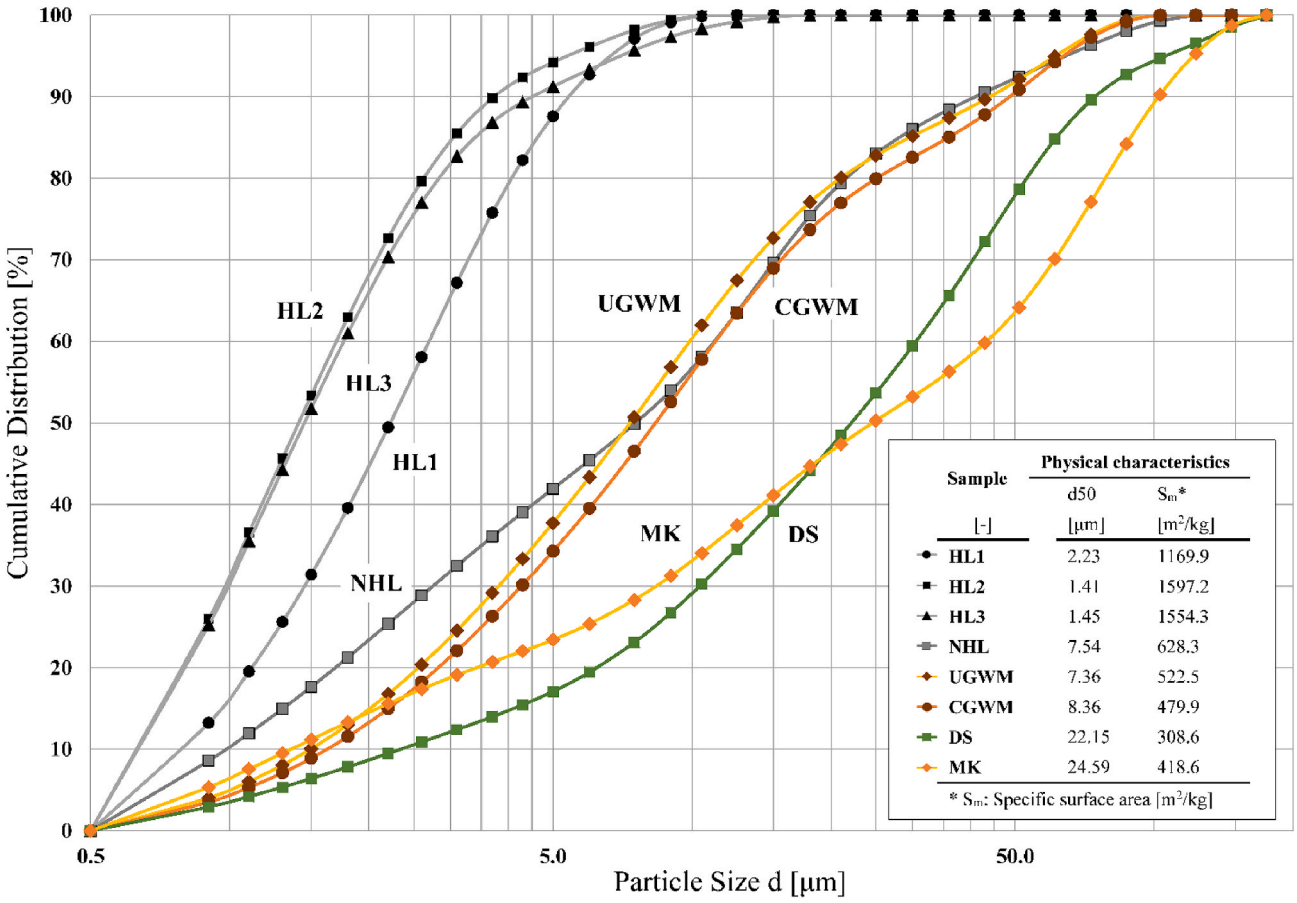

Fig. 1. Particle size distribution and physiochemical characteristics of applied materials: HL1, HL2, HL3, UGWM, CGWM (calcined at 850 °C), DS and MK powders.

UGWM due to clumping effect of the clay particles from the compaction of the minerals when exposed to high temperatures (850 °C). MK and DS show comparatively coarser grain size distributions with average particle sizes of 22.15 µm resp. 24.49 µm and specific surface 308.6.9 m^2/kg resp. 479.9 m^2/kg. The different raw materials cover a wide range of particle size distributions, which suggests a compact packing density of the mixes between the different constituents of the lime-MK-GWM pastes [49–51].

3.2. Mineralogy and thermal analysis of the primary materials

XRD patterns of the UGWM and the CGWM are presented in Fig. 2. The GWM powders indicate a strong reflection of quartz, medium peak intensities of muscovite, illite and kaolinite, and poor diffraction peaks of hematite. Traces of the phase shifts of kaolinite to XRD amorphous phases can be observed in the X-ray diffraction pattern of the UGWM and CGWM powders [13,14]. The quantitative XRD analysis of all the investigated materials is summarized in Table 3. The quantitative mineralogical evaluation, following the method described in Refs. [14, 52], confirms for the GWM powders the high presence of amorphous components and the major crystalline phase as quartz, followed by muscovite, illite and kaolinite as medium phases and hematite respectively $KAl_3Si_3O_{11}$ as minor phases. Further comparison reveals the positive impact of thermal treatment (calcination) on the GWM powders, as a clear rise of the amorphous content results from the transition of kaolinite to XRD amorphous phases. In addition, a slight decrease in illite content and a phase transition of muscovite phases into $KAl_3Si_3O_{11}$ can be observed. Comparatively, the used metakaolin (MK) is majorly XRD amorphous with some content of quartz, which explains the high pozzolanicity of the commercial product. The hydrated lime powders HL1-HL3 consist primarily of portlandite (calcium hydroxide) and thereby also confirm the findings of the chemical analysis. The low

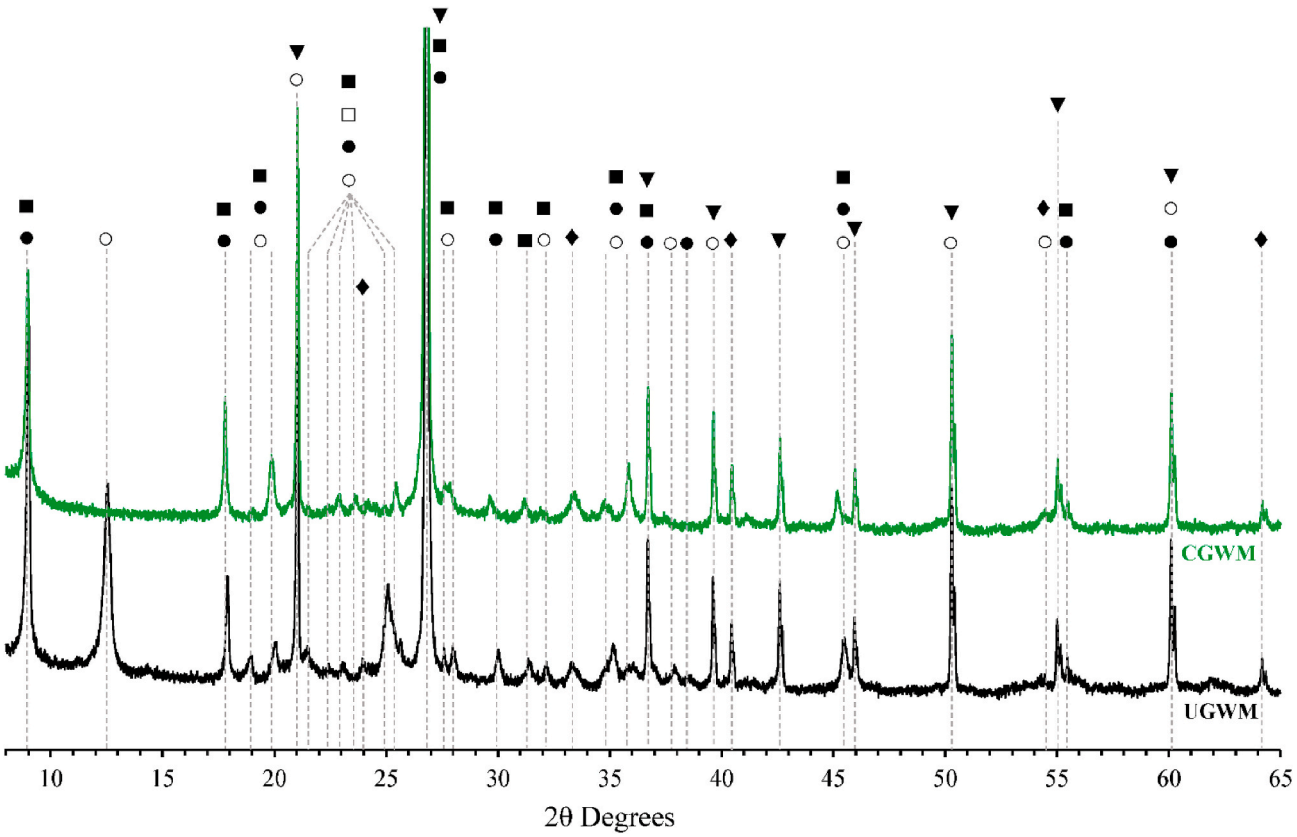

Fig. 2. X-ray diffractogram of UGWM and CGWM: ▼ - Quartz, ■ - Muscovite, ● - Illite, ○ - Kaolinite, ◆ - Hematite, □ - $KAl_3Si_3O_{11}$.

Table 3
Mineralogical composition of NHL, HL1-3, DS, MK, UGWM and CGWM powders.

Sample	Mineralogical composition [%]						
	Quartz[a]	Muscovite	Illite	Kaolinite	Hematite	$KAl_3Si_3O_{11}$	Amorph
UGWM	35.0	15.3	10.9	11.9	1.0	1.3	24.5
CGWM	35.0	8.4	12.8	0.5	2.2	7.0	34.1

	Portlandite	Calcite	Dolomite	Mica	Quartz	Amorph
HL1	92.5	7.5	–	–	–	–
HL2	98.9	1.1	–	–	–	–
HL3	99.2	0.8	–	–	–	–
DS	–	0.5	72.4	10.4	16.7	–
MK	–	–	–	–	31.2	68.8

	C_3S	C_2S	C_3A	C_4AF	Calcite	Portlandite	Anhydrite	Peri.[b]	Quartz	D.[b]	Amorph
NHL	12.2	17.9	2.8	2.8	28.1	29.8	0.1	0.4	2.6	0.4	2.9

[a] Quartz content fixed as standard.
[b] Peri. – Periclase and D. - Dolomite.

calcite amounts can be explained either as remainders from the original limestone ($CaCO_3$) or as a result of carbonation of hydrated lime [53]. The main mineralogical phases observed for NHL were high contents of portlandite and calcite ($CaCO_3$), and medium contents of alite (C_3S) and belite (C_2S).

3.3. Compressive strength tests of hardened specimens

3.3.1. Natural hydraulic lime vs hydrated lime

Fig. 3 presents the results of the compressive strength test performed on the hardened prismatic specimens of the first series (S1) at 7, 14 and 28 days. The gradual gain in compressive strength for each mixing proportion over the investigated curing age validates the assumption that a strengthening structure is developed and thus the potential of lime-MK pastes using untreated, pure GWM as alternatives to cement-based products for construction applications. Overall, the mechanical strengths of the hardened pastes containing hydrated lime were higher than the strengths achieved by the mixtures containing natural hydraulic lime for all mixtures and curing ages, except for PGC_NHL at 7 days. The highest 28-day compressive strength of 13.3 MPa was achieved by hardened pastes containing hydrated lime, namely PGB_HL1, whereas the highest mechanical strength for hardened pastes containing natural hydraulic lime was reached by PGC_HL3 with 9.8 MPa.

Furthermore, for the hardened pastes containing hydraulic lime, on average around 70% of the 28-day compressive strength was already reached at 7 days of curing age due to predominant hydration reaction of hydraulic lime with formation of stable calcium silicate hydrate (CSH) phases over the first days [25,33]. The progressive development of additional CSH phases from pozzolanic reaction could not be traceably observed, mainly due to the lower availability of free calcium hydroxide

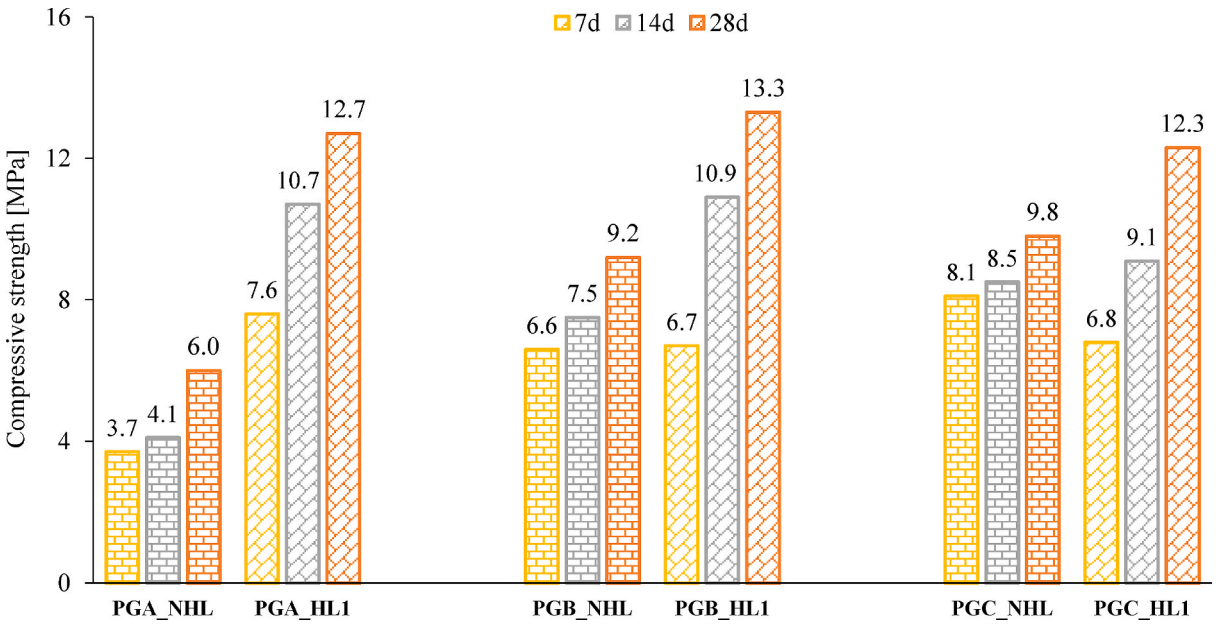

Fig. 3. Development of the mechanical properties of hardened pastes from three different mixtures containing PGWM, MK, DS, and NHL or HL1.

in the binder system in opposition to the presence of high reactive MK and low reactive PGWM. In comparison, for the mixtures containing hydrated lime only about 55% of the 28-day compressive strength was achieved over the same time period (7 days). The hardening process of the hydrated lime-based pastes consists primarily of the formation of solid calcium silicate hydrates which are formed from the pozzolanic reaction between calcium hydroxide and the reactive aluminosilicate minerals in the first hours and days [54]. Simultaneously, an additional increase in strength is considered due to the development of further reaction products from carbonation reaction with increasing hardening ages [30,53]. However, the strength-enhancing properties of pure GWM could not be identified, mainly due to its incorporation in the mixtures in its very low-reactive and untreated raw state.

The strength evolution of the hardened pastes of S1 validates the continuous hardening reactions of lime-MK pastes using pure GWM until 28 days of curing and the higher mechanical performances of mixtures using hydrated lime instead of hydraulic lime.

3.3.2. *Variation of the composition of hydrated lime*

The compressive strength results at 7, 14, 28 and 90 days of the hardened lime-MK pastes containing PGWM and different hydrated limes (HL1, HL2 and HL3) with the same mixing proportion are presented in Fig. 4. As expected, the hardened pastes of the second series (S2) show very similar profile of strength gain with a gradual growth in compressive strength with increasing curing age. The strength evolution of HL2 and HL3 are almost identical, whereas HL1 shows a slightly lower strength development over the same period of time. All hardened pastes achieve compressive strengths slightly above 10 MPa at 28 days; however, at 90 days of curing age, the hardened pastes containing HL2 and HL3 reach highest mechanical strengths of 13.4 MPa, respectively, 13.3 MPa, whereas hardened pastes containing HL1 achieve maximal compressive strength of 11.5 MPa. One explanation could be the lower

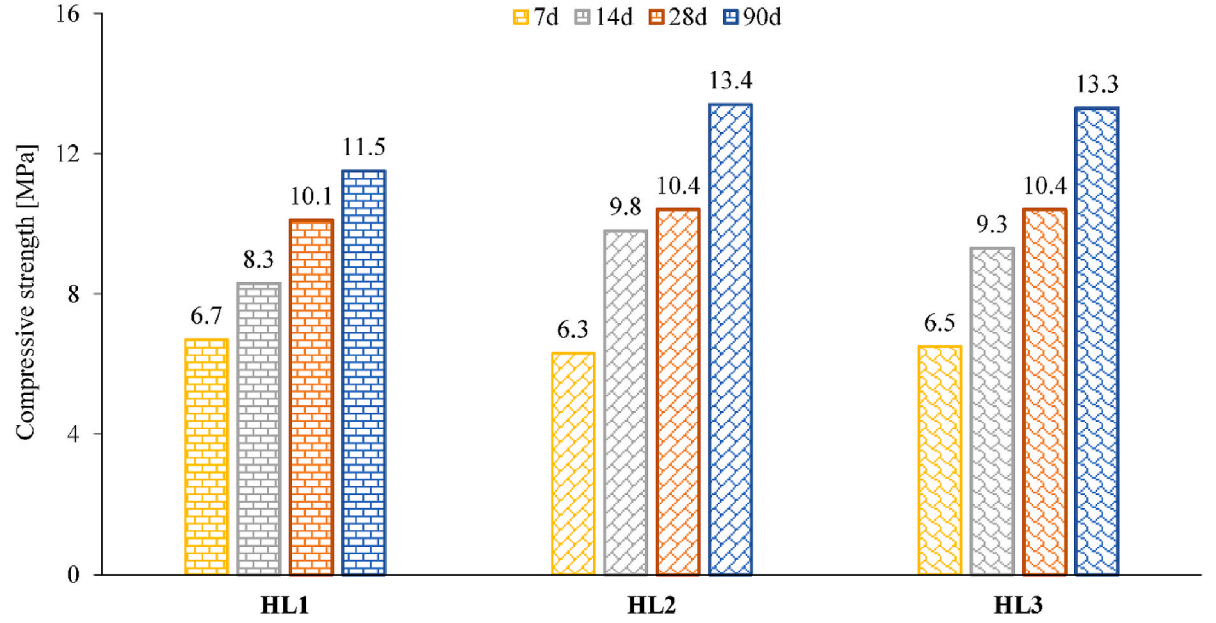

Fig. 4. Development of the mechanical properties of hardened pastes containing PGWM, MK, DS, and HL1, HL2 or HL3.

free calcium hydroxide content in HL1 as presented in Tables 2 and 3, leading to lower compressive strength gains from advancing pozzolanic reactions and carbonation to later curing ages. The strength evolution of the hardened pastes of S2 confirms the potential of hardened lime-MK pastes using pure GWM and hydrated lime to achieve promising mechanical performances from hydration, pozzolanic and carbonation reactions. Nonetheless, no clear influence of the addition of pure GWM on the reaction kinetics of the pastes and the resulting performances could be deducted. Therefore, the third series of mixtures was prepared and examined to assess the influence of incorporating uncalcined and calcined GWM powders on the performance of lime-MK binders.

3.3.3. *Varying mixture design and use of UGWM and CGWM*

Fig. 5 and Fig. 6 present the compressive strength results at curing ages of 7, 28, 56 and 90 days performed on the hardened pastes of the third series of mixtures. Fig. 5 shows the compressive strength values of hardened pastes containing uncalcined GWM (UGWM) powders and Fig. 6 illustrates the mechanical strength values of the hardened pastes of the same mixing proportions containing calcined GWM (CGWM). The control specimen without GWM content (REF) reaches the highest 7-day compressive strength of 8.3 MPa among all the investigated mixtures, resulting from the early formation of calcium silicate hydrate phases from the pozzolanic reactions between the high reactive MK and the free calcium hydroxide. At curing ages up to 56 days, REF gradually increases in strength until a clear drop of the mechanical performance can be observed at 90 days. All tested specimens, except REF at 90 days and CG_1:1.33:1 at 56 days, show an increasing profile of compressive strengths with increasing curing age up to 90 days. After 56 days of curing, the observed decrease in compressive strength of REF could be explained by the high lime content in the reference paste, leading to further carbonation of $Ca(OH)_2$ [31] and CSH phases (instability of the formed calcium silica hydrates) [55–57] as well as due to drying shrinkage (micro-cracking) and carbonation shrinkage induced strength losses [58,59]. Following the evolution of strength, the early reaction products are predominately resulting from the formation of calcium silicate hydrates from pozzolanic reactions of the active phases of the amorphous aluminosilicate precursors with the initial free calcium hydroxide. Due to the presence of the reactive pozzolan and the dominance of the pozzolanic reactions in the wet conditions at early curing ages, the carbonation reaction occurs from 28 days onwards. Furthermore, the carbonation of the remaining free lime drove forward further strength development and simultaneously additional networks of pozzolanic hydrates slowly formed above 28 days of curing age [25].

As expected, similar to the use of PGWM, the incorporation of UGWM in the lime-MK mixtures (Fig. 5) did not show any clear improvement in the mechanical performances of the hardened pastes (maximal compressive strength of 13.8 MPa at 90 days by CG_1:1.33:1) compared to the reference mixture. The mechanical strength increased only slightly from 28 to 90 days for all hardened pastes. As concluded in the investigations carried out in Ref. [13,14], without additional thermal processing (calcination), GWM powders show very low pozzolanicity and therefore, the addition of UGWM lead to a dilution effect on the available reactive aluminosilicate materials in the pastes, leading to a lower rate of early pozzolanic reactions of MK and free calcium hydroxide.

Nonetheless, the incremental strength development pattern of all the lime-MK-UGWM pastes, compared to the already observed strength drop of the reference sample at 90 days of curing age, suggests that higher lime content (more unreacted calcium hydroxide) in the binder proportions result in significant strength losses at longer curing ages [33].

As shown in Fig. 6, for the same mixing proportions, significantly higher compressive strength values were obtained by the lime-MK-CGWM pastes than by lime-MK-UGWM pastes at all curing ages. In contrast to the lime-MK-UGWM pastes, the incorporation of the CGWM powders did not hinder the pozzolanic activity of the aluminosilicate materials of the mixtures. The highest compressive strength of 18.8 MPa was achieved by CG_1:1.66:1 at 90 days of curing age compared to 13.8 MPa by UG_1:1.66:1 (compressive strength gain of 36%). The phase transition of GWM into a stable and more amorphous meta-state after thermal treatment at 850 °C as well as the finer granulometry of the CGWM powder compared to the MK powder explain the strongly positive pozzolanic activity of MK-CGWM combination leading to the overall compressive strength improvements. Furthermore, the strength-based evaluations show that the improved mechanical performance is not directly related to the increasing MK content and/or CGWM content, but rather depends on the interrelated combinations of the ternary mixing proportions considering the lime:pozzolan ratio as well as the CGWM: MK ratio. The highest compressive strengths were observed for

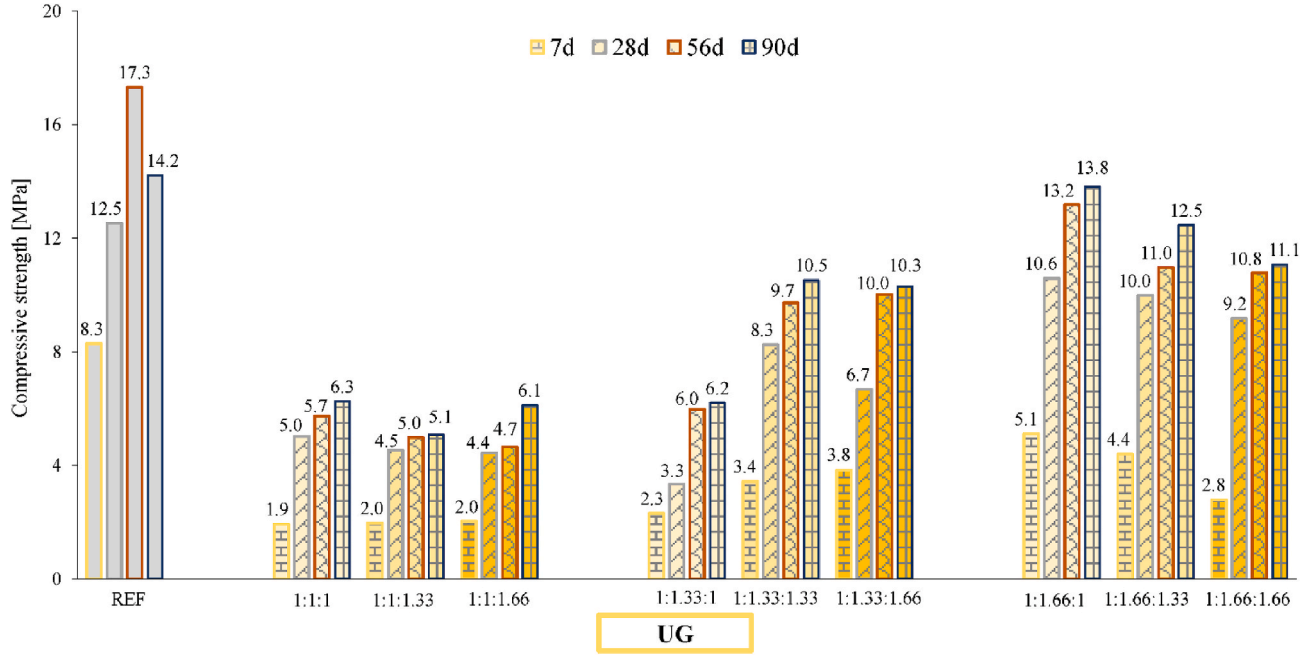

Fig. 5. Development of the mechanical properties of hardened pastes containing UGWM, HL2, MK and DS.

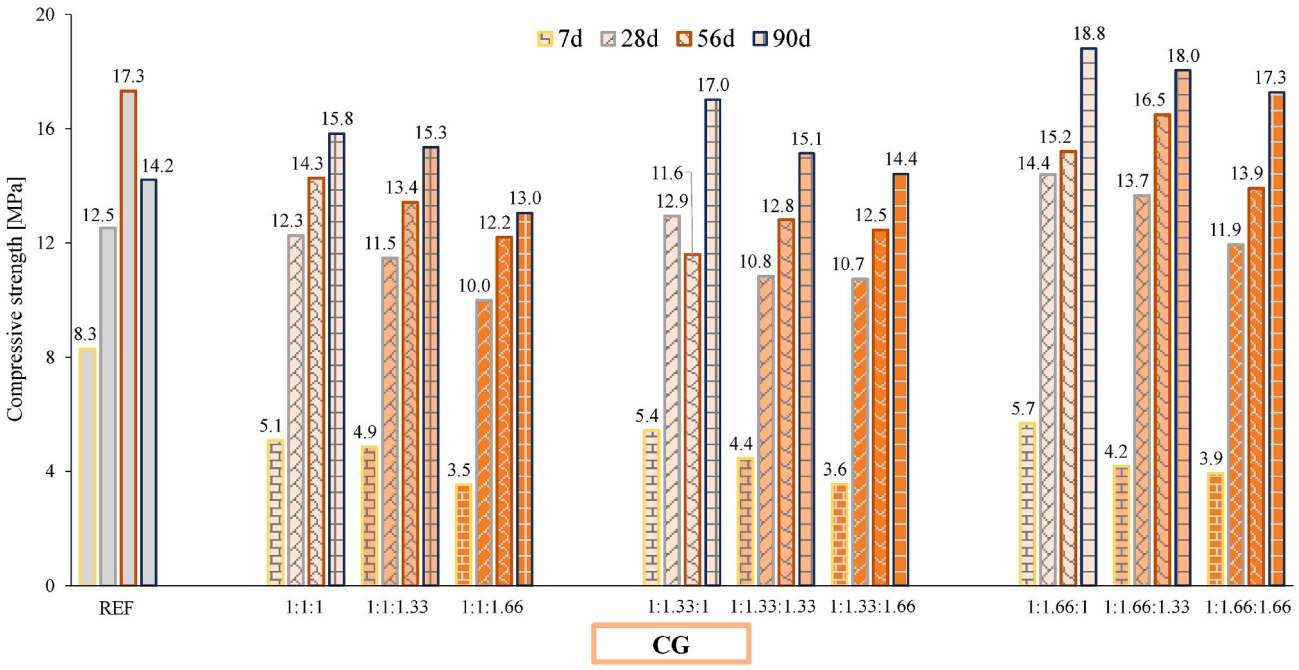

Fig. 6. Development of the mechanical properties of hardened pastes containing CGWM, HL2, MK and DS.

hardened lime-MK-CGWM pastes with lime:pozzolan ratios of 0.3–0.42 and CGWM:MK ratios of 0.6–1.0.

3.4. Phase composition of the hardened specimens by STA

The evolution of the STA curves of the hardened specimen CG_1:1.66:1 is illustrated in Fig. 7. The mass loss and the heat flow variation of the sample is monitored from ambient temperature up to 1000 °C. A total mass drop of 24.13% can be observed following the TGA curve over the investigated temperature range. Three separate mass reduction segments can be pointed out, each segment can be attributed to a specific nature change (mass change in combination with endothermic and exothermic reactions) within the specimen: The first segment of gradual mass loss (−3.16%) can be perceived at a temperature of 250 °C. This reduction represents the evaporation of the bound waters of the formed calcium silicate hydrates as products from the pozzolanic reactions and the absorbed water of calcium hydroxide as well as the burning of organic and/or volatile components. The second mass loss range (−1.55%) can be perceived from 250 °C to 550 °C due to decomposition of the AFm phases and calcium aluminate hydrate (CAH) phases, and the dehydroxylation of calcium hydroxide. The largest mass reduction from around 700 °C up to about 800 °C is mainly driven by the

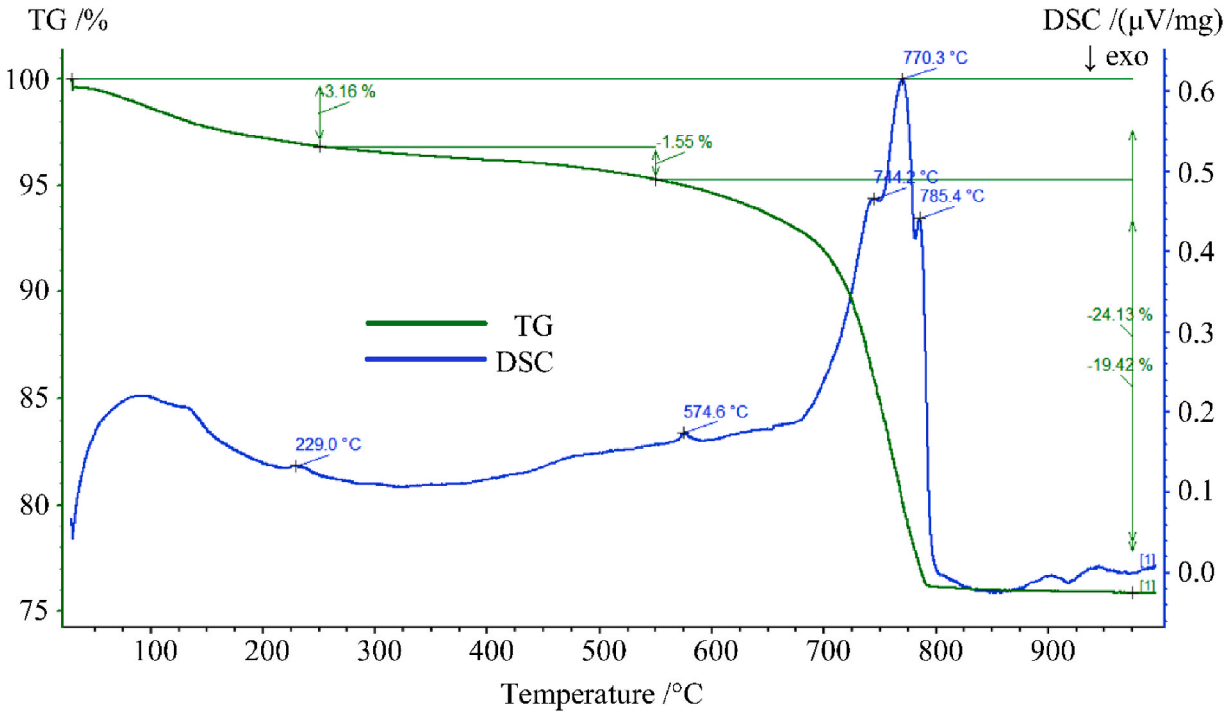

Fig. 7. STA (TG-DSC) analysis of hardened specimen of CG_1:1.66:1.

decarbonation of calcite ($CaCO_3$) in the hardened pastes until a constant mass state is reached. The corresponding DSC curve confirms the dehydration process of the different CSH products by the endothermic peak at about 230 °C, then the endothermic peak at 574.6 °C corresponds to the phenomenon of quartz inversion (dolomitic sand) and the endothermic peaks observed between 740 °C and 790 °C can be attributed to the decarbonation of $CaCO_3$. These peaks confirm the carbonation reaction of free calcium hydroxide with CO_2 from air, leading to the formation of calcium carbonate ($CaCO_3$). Overall, the findings of the STA analysis are consistent with the results of the compressive strength test and confirm the formation of CSH phases (pozzolanic products) as well as the formation of $CaCO_3$ (carbonation products) as the dominant chemical reaction mechanisms of lime-MK-CGWM pastes.

3.5. Microstructural analysis

Scanning electron microscopy (SEM) was carried out on fractured samples to examine the resulting microstructural configurations of selected pastes after 56 days of curing age. Fig. 8a presents the microstructure of a natural hydraulic lime-MK-PGWM paste (PCB_NHL), whereas Fig. 8b–e illustrate the SEM micrographs of PCB_HL1, a hydrated lime-MK paste with PGWM. Fig. 8a shows that medium quantities of reaction products were formed and a partially condensed microstructure was built with several visible cracks and micro gaps. In comparison, Fig. 8b depicts a much denser structure with significant amount of amorphous compound forming a compact bond between the reaction products and the quartz particles. As expected, these SEM observations are consistent with the results of the compressive strength evaluation. Fig. 8c confirms that the formation of a dense network of CSH phases as a result of a pozzolanic reaction between free lime and the

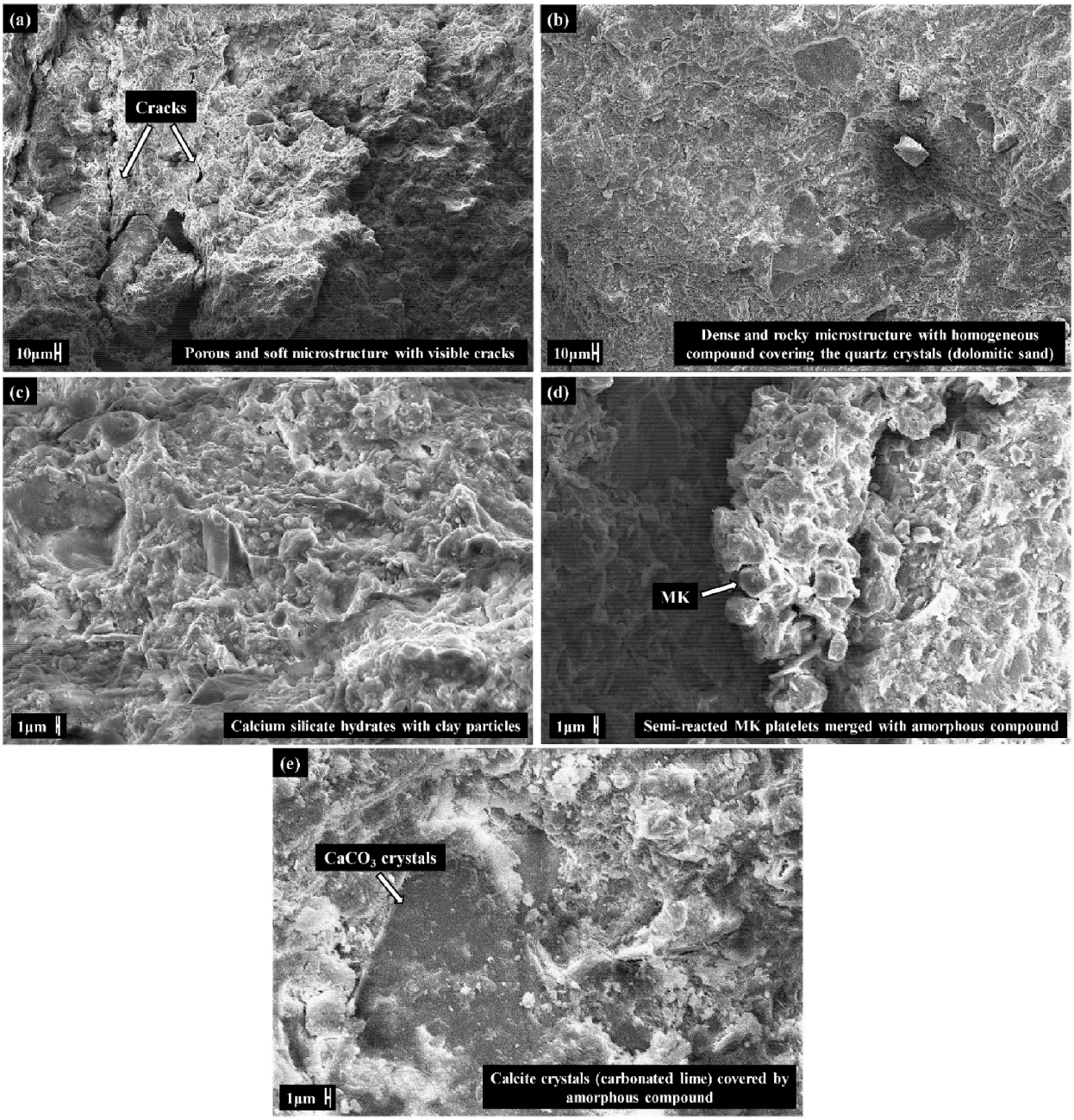

Fig. 8. SEM micrographs of (a) PGB_NHL and (b)–(e) PGB_HL1 at curing age of 56 days.

aluminosilicate raw materials. In the SEM micrographs (Fig. 8d), amorphous cement-like compounds can be observed as well as traces of unreacted and reacted clay particles. Plate-like mineral formations indicate the presence of unreacted or semi-reacted metakaolinite. Moreover, some calcite crystals, resulting from the carbonation of lime, were observed, covered by the reaction products (Fig. 8e), which confirms the strengthening capacities of the lime-pozzolan binder matrix by carbonation.

Overall, for the pastes using hydrated limes, a dense, homogenous microstructural composition between the aluminosilicate-rich compounds (clay minerals) and the reaction products was observed. This compact bond indicates that strong reaction products from pozzolanic reaction between GWM-MK and the hydrated lime were successfully synthesised. The formed binder matrix seems to be slightly weaker than that of usual cement-based pastes [28,60,61]. However, very promising compressive strength results show the benefit of using hydrated lime in combination with GWM powders to improve the microstructural configuration of the binders. Finally, some unreacted aluminosilicate constituents were observed in almost every sample, which suggest that further optimization of the mixing proportions of the applied quantities of each components could significantly enhance the properties of the ternary lime-MK-GWM pastes.

4. Conclusions

In this work, an aluminosilicate-rich raw material, namely GWM powder, was incorporated in lime-based pastes to evaluate its strength-enhancing potential. Large varieties of lime-MK-GWM pastes with very promising mechanical properties were presented. From the presented results, considering the varying mixing proportions, the use of different types of lime powders, and GWM at different treatment levels, the following conclusions can be drawn from this study:

- XRD data indicate the beneficial effect of thermal treatment (calcination) on the mineralogy of GWM powders with a clear increase in amorphous content, resulting from the transition of kaolinite to metakaolin. The used metakaolin (MK) shows a very high amorphous content with a medium content of quartz. These findings indicate that both raw materials could exhibit medium to high pozzolanicity.
- For both hydraulic and hydrated lime systems, acceptable strengths for constructive applications were developed over the investigated curing ages. Considering the achieved mechanical performances, the use of hydrated lime is recommended instead of natural hydraulic lime as more dense and strength-enhancing reaction products from pozzolanic reaction were formed at early curing ages.
- The STA analysis as well as the SEM analysis of the microstructure confirm the presence of the CSH phases and calcite ($CaCO_3$) as major reaction products.
- The examination of over 250 hardened specimens with varying lime-MK-GWM proportions and different curing ages suggests that the only consideration of the 28-day compressive strength as it is the case for traditional cement-based products is not recommendable for the lime-pozzolan binder systems due to the involved slower pozzolanic reaction and carbonation reaction processes compared to the early hydration reaction.
- The highest compressive strength of 18.8 MPa was achieved by CG_1:1.66:1 at 90 days and the strength-based evaluation presents the use of calcined GWM as a very effective pozzolan in the ternary lime-MK-GWM binder systems. The achieved performances suggest that this composite concept can be considered as a potential low-to medium-strength material for construction applications.

Finally, the results of this study will contribute to further enrichment of investigations on waste materials as powerful SCMs as well as consequently promote their incorporation in lime-pozzolan binder systems. The establishment of calcined GWM as a competitive and alternative pozzolan requires further optimizations of the binder concepts, the analysis of long-term behaviour of the binder systems, and durable solutions regarding its full scalability into industrial processes need to be developed. It is important to divert existing waste management flows by stimulating optimization and innovation in the revalorisation of waste materials to limit the use of landfilling and to replace the “end-of-life” concept of industrial co-products by reusing or recycling them as raw materials. This will bring double benefit to environment as waste is eliminated from one system and later is used as a resource in another system.

Declaration of competing interest

The authors declare that they have no known competing financial interests or personal relationships that could have appeared to influence the work reported in this paper.

Acknowledgements

The authors wish to acknowledge Carrières Feidt S.A for the supply of the gravel wash mud (GWM) and Contern S.A. for the supply of the different limes, metakaolin and the dolomitic sand used in this work. The authors would like to express their gratitude to Dr. Claude Simon from Cimalux S.A. and Dr. Marcus Paul from the Wilhelm Dyckerhoff Institut (WDI) for their valuable contributions to the applied characterisation techniques, and Dr. Oscar Baeza-Urrea from University of Trier for the scanning electron microscopy.

References

[1] M. Gimenez, CO2 uses in the cement industry, Carbon Capture Util. Storage - SETIS. (2016) 34–35, https://doi.org/10.1007/978-3-030-30908-4_5.
[2] R.M. Andrew, Global CO2 emissions from cement production, Earth Syst. Sci. Data 10 (2018) 195–217, https://doi.org/10.5194/essd-10-195-2018.
[3] R.M. Andrew, Global CO2 emissions from cement production, 1928 – 2017, Earth Syst. Sci. Data 10 (2018) 2213–2239, https://doi.org/10.5194/essd-10-2213-2018.
[4] Ecofys, Methodology for the free allocation of emission allowances in the EU ETS post 2012 - sector report for the lime industry. https://ec.europa.eu/clima/sites/clima/files/ets/allowances/docs/bm_study-lime_en.pdf, 2009. (Accessed 6 July 2020).
[5] WBCSD Cement Sustainability Initiative, Getting the numbers right - GCCA in NumbeRs, GNR proj. Report. CO2. https://www.wbcsdcement.org/index.html, 2017. (Accessed 3 April 2020).
[6] V.M. Malhotra, P.K. Mehta, Pozzolanic and Cementitious Materials 1 (1996).
[7] M.C.G. Juenger, R. Siddique, Recent advances in understanding the role of supplementary cementitious materials in concrete, Cem. Concr. Res. (2015) 71–80, https://doi.org/10.1016/j.cemconres.2015.03.018, cli.
[8] P. Suraneni, J. Weiss, Examining the pozzolanicity of supplementary cementitious materials using isothermal calorimetry and thermogravimetric analysis, Cement Concr. Compos. 83 (2017) 273–278, https://doi.org/10.1016/j.cemconcomp.2017.07.009.
[9] S. Ferreiro, D. Herfort, J.S. Damtoft, Effect of raw clay type, fineness, water-to-cement ratio and fly ash addition on workability and strength performance of calcined clay – limestone Portland cements, Cement Concr. Res. 101 (2017) 1–12, https://doi.org/10.1016/j.cemconres.2017.08.003.
[10] S. Samad, A. Shah, Role of binary cement including Supplementary Cementitious Material (SCM), in production of environmentally sustainable concrete: a critical review, Int. J. Sustain. Built Environ. 6 (2017) 663–674, https://doi.org/10.1016/j.ijsbe.2017.07.003.
[11] R. Walker, S. Pavía, Physical properties and reactivity of pozzolans, and their influence on the properties of lime-pozzolan pastes, Mater. Struct. 44 (2011) 1139–1150, https://doi.org/10.1617/s11527-010-9689-2.
[12] R.T. Thorstensen, P. Fidjestol, Inconsistencies in the pozzolanic strength activity index (SAI) for silica fume according to EN and ASTM, Mater. Struct. Constr. 48 (2015) 3979–3990, https://doi.org/10.1617/s11527-014-0457-6.
[13] V.B. Thapa, D. Waldmann, J.-F. Wagner, A. Lecomte, Assessment of the suitability of gravel wash mud as raw material for the synthesis of an alkali-activated binder, Appl. Clay Sci. 161 (2018) 110–118, https://doi.org/10.1016/j.clay.2018.04.025.
[14] V.B. Thapa, D. Waldmann, C. Simon, Gravel wash mud, a quarry waste material as supplementary cementitious material (SCM), Cem, Concr. Res. 124 (2019) 105833, https://doi.org/10.1016/j.cemconres.2019.105833.
[15] A. Seco, F. Ramirez, L. Miqueleiz, P. Urmeneta, B. Garcia, E. Prieto, V. Oroz, in: K.-Y. Show, G. Xinxin (Eds.), Types of Waste for the Production of Pozzolanic Materials – A Review, Ind. Waste, IntechOpen, Rijeka, 2012, pp. 141–150, https://doi.org/10.5772/36285.

[16] K. Scrivener, F. Martirena, S. Bishnoi, S. Maity, Calcined clay limestone cements (LC3), Cement Concr. Res. 114 (2017) 49–56, https://doi.org/10.1016/j.cemconres.2017.08.017.
[17] B.B. Sabir, S. Wild, J. Bai, Metakaolin and calcinded clays as pozzolans for concrete: a review, Cement Concr. Compos. 23 (2001) 441–454.
[18] H. Yanguatin, J. Tobón, J. Ramírez, Pozzolanic reactivity of kaolin clays, Review 32 (2017) 13–24.
[19] Y. Zhou, J. Li, J. xin Lu, C. Cheeseman, C.S. Poon, Sewage sludge ash: a comparative evaluation with fly ash for potential use as lime-pozzolan binders, Construct. Build. Mater. 242 (2020) 118160, https://doi.org/10.1016/j.conbuildmat.2020.118160.
[20] R.L. Day, C. Shi, Influence of the fineness of pozzolan on the strength of lime natural-pozzolan cement pastes, Cement Concr. Res. 24 (1994) 1485–1491, https://doi.org/10.1016/0008-8846(94)90162-7.
[21] J. Cabrera, M.F. Rojas, Mechanism of hydration of the metakaolin-lime-water system, Cement Concr. Res. 31 (2001) 177–182, https://doi.org/10.1016/S0008-8846(00)00456-7.
[22] A.L. Gameiro, A.S. Silva, M. do R. Veiga, A.L. Velosa, Lime-metakaolin hydration products: a microscopy analysis, Mater. Technol. 46 (2012) 145–148.
[23] A. Gameiro, A. Santos Silva, R. Veiga, A. Velosa, Hydration products of lime-metakaolin pastes at ambient temperature with ageing, Thermochim. Acta 535 (2012) 36–41, https://doi.org/10.1016/j.tca.2012.02.013.
[24] E. Aggelakopoulou, A. Bakolas, A. Moropoulou, Properties of lime-metakolin mortars for the restoration of historic masonries, Appl. Clay Sci. 53 (2011) 15–19, https://doi.org/10.1016/j.clay.2011.04.005.
[25] E.R. Grist, K.A. Paine, A. Heath, J. Norman, H. Pinder, Compressive strength development of binary and ternary lime-pozzolan mortars, Mater. Des. 52 (2013) 514–523, https://doi.org/10.1016/j.matdes.2013.05.006.
[26] A. Sepulcre-Aguilar, F. Hernández-Olivares, Assessment of phase formation in lime-based mortars with added metakaolin, Portland cement and sepiolite, for grouting of historic masonry, Cement Concr. Res. 40 (2010) 66–76, https://doi.org/10.1016/j.cemconres.2009.08.028.
[27] G. Matias, P. Faria, I. Torres, Lime mortars with heat treated clays and ceramic waste: a review, Construct. Build. Mater. 73 (2014) 125–136, https://doi.org/10.1016/j.conbuildmat.2014.09.028.
[28] B.A. Silva, A.P. Ferreira Pinto, A. Gomes, Natural hydraulic lime versus cement for blended lime mortars for restoration works, Construct. Build. Mater. 94 (2015) 346–360, https://doi.org/10.1016/j.conbuildmat.2015.06.058.
[29] A. Vimmrová, M. Keppert, O. Michalko, R. Černý, Calcined gypsum-lime-metakaolin binders: design of optimal composition, Cement Concr. Compos. 52 (2014) 91–96, https://doi.org/10.1016/j.cemconcomp.2014.05.011.
[30] V. Nezerka, Microstructure, Chemical Processes and Experimental Investigation of Lime-Based Mortars, 2012, p. 26.
[31] A.S. Silva, A. Gameiro, J. Grilo, R. Veiga, A. Velosa, Long-term behavior of lime-metakaolin pastes at ambient temperature and humid curing condition, Appl. Clay Sci. 88–89 (2014) 49–55, https://doi.org/10.1016/j.clay.2013.12.016.
[32] A. Gameiro, A. Santos Silva, P. Faria, J. Grilo, T. Branco, R. Veiga, A. Velosa, Physical and chemical assessment of lime-metakaolin mortars: influence of binder: aggregate ratio, Cement Concr. Compos. 45 (2014) 264–271, https://doi.org/10.1016/j.cemconcomp.2013.06.010.
[33] J. Grilo, A. Santos Silva, P. Faria, A. Gameiro, R. Veiga, A. Velosa, Mechanical and mineralogical properties of natural hydraulic lime-metakaolin mortars in different curing conditions, Construct. Build. Mater. 51 (2014) 287–294, https://doi.org/10.1016/j.conbuildmat.2013.10.045.
[34] G. Matias, P. Faria, I. Torres, Lime mortars with ceramic wastes: characterization of components and their influence on the mechanical behaviour, Construct. Build. Mater. 73 (2014) 523–534, https://doi.org/10.1016/j.conbuildmat.2014.09.108.
[35] M. Jerman, V. Tydlitát, M. Keppert, M. Čáchová, R. Černý, Characterization of early-age hydration processes in lime-ceramic binders using isothermal calorimetry, X-ray diffraction and scanning electron microscopy, Thermochim. Acta 633 (2016) 108–115, https://doi.org/10.1016/j.tca.2016.04.005.
[36] M.S. Morsy, A.M. Rashad, H. Shoukry, M.M. Mokhtar, S.A. El-Khodary, Development of lime-pozzolan green binder: the influence of anhydrous gypsum and high ambient temperature curing, J. Build. Eng. 28 (2020) 101026, https://doi.org/10.1016/j.jobe.2019.101026.
[37] R.M.H. Lawrence, T.J. Mays, P. Walker, D. D'Ayala, Determination of carbonation profiles in non-hydraulic lime mortars using thermogravimetric analysis, Thermochim. Acta 444 (2006) 179–189, https://doi.org/10.1016/j.tca.2006.03.002.
[38] J. Lanas, J.L.P. Bernal, M.A. Bello, J.I.A. Galindo, Mechanical properties of natural hydraulic lime-based mortars, Cement Concr. Res. 34 (2004) 2191–2201, https://doi.org/10.1016/j.cemconres.2004.02.005.
[39] A. Bakolas, E. Aggelakopoulou, A. Moropoulou, S. Anagnostopoulou, Evaluation of pozzolanic activity and physicomechanical characteristics in metakaolin-lime pastes, J. Therm. Anal. Calorim. 84 (2006) 157–163, https://doi.org/10.1007/s10973-005-7262-y.
[40] G. Matias, P. Faria, I. Torres, Lime mortars with heat treated clays and ceramic waste: a review, Construct. Build. Mater. 73 (2014) 125–136, https://doi.org/10.1016/j.conbuildmat.2014.09.028.
[41] EN 459-1:2010, Building Lime - Part 1: Definitions, Specifications and Conformity Criteria, European Committee for standardization, 2010.
[42] NF P18-513:2012-08-01, Addition for Concrete - Metakaolin - Specifications and Conformity Criteria, AFNOR, 2012.
[43] DIN EN 196-1:2016-11, Methods of Testing Cement - Part 1: Determination of Strength, European Committee for standardization, 2016.
[44] R.W. Cheary, A.A. Coelho, J.P. Cline, Fundamental Parameters Line Profile Fitting in Laboratory Diffractometers, vol. 109, 2004, pp. 1–25, https://doi.org/10.6028/jres.002.
[45] A.H. De Aza, A.G. De La Torre, M.A.G. Aranda, F.J. Valle, S. De Aza, Rietveld Quantitative Analysis of Buen Retiro Porcelains 87 (2004) 449–454, https://doi.org/10.1111/j.1551-2916.2004.00449.x.
[46] M. Paul, D. Ag, W. Dyckerhoff, Application of the Rietveld Method in the Cement Industry, 2005, pp. 1–3.
[47] H.M. Rietveld, A profile refinement method for nuclear and magnetic structures, J. Appl. Crystallogr. 2 (1969) 65–71, https://doi.org/10.1107/S0021889869006558.
[48] H.M. Rietveld, The Rietveld Method : a retrospection 225 (2010) 545–547, https://doi.org/10.1524/zkri.2010.1356.
[49] I. Mehdipour, A. Kumar, K.H. Khayat, Rheology, hydration, and strength evolution of interground limestone cement containing PCE dispersant and high volume supplementary cementitious materials, Mater. Des. 127 (2017) 54–66, https://doi.org/10.1016/j.matdes.2017.04.061.
[50] H. Moosberg-Bustnes, B. Lagerblad, E. Forssberg, The function of fillers in concrete, Mater. Struct. Constr. 37 (2004) 74–81, https://doi.org/10.1617/13694.
[51] J. Tangpagasit, R. Cheerarot, C. Jaturapitakkul, K. Kiattikomol, Packing effect and pozzolanic reaction of fly ash in mortar, Cement Concr. Res. 35 (2005) 1145–1151, https://doi.org/10.1016/j.cemconres.2004.09.030.
[52] M. Paul, Quality Control of Autoclaved Aerated Concrete by Means of X-Ray Diffraction, 2018, pp. 111–116, https://doi.org/10.1002/cepa.894.
[53] M. Erans, S.A. Nabavi, V. Manović, Carbonation of lime-based materials under ambient conditions for direct air capture, J. Clean. Prod. 242 (2020), https://doi.org/10.1016/j.jclepro.2019.118330.
[54] J.G. Cabrera, M. Frías, Mechanism of hydration of the metakaolin -lime-water system, Cement Concr. Res. 31 (2001) 177–182.
[55] K. Suzuki, T. Nishikawa, S. Ito, Formation and carbonation of C-S-H in water, Cement Concr. Res. 15 (1985) 213–224, https://doi.org/10.1016/0008-8846(85)90032-8.
[56] P.A. Slegers, P.G. Rouxhet, Carbonation of the hydration products of tricalcium silicate, Cement Concr. Res. 6 (1976) 381–388, https://doi.org/10.1016/0008-8846(76)90101-0.
[57] K. Kobayashi, K. Suzuki, Y. Uno, Carbonation of concrete structures and decomposition of CSH, Cement Concr. Res. 24 (1994) 55–61, https://doi.org/10.1016/0008-8846(94)90082-5.
[58] H. Ye, A. Radlińska, J. Neves, Drying and carbonation shrinkage of cement paste containing alkalis, Mater. Struct. Constr. 50 (2017), https://doi.org/10.1617/s11527-017-1006-x.
[59] E.G. Swenson, P.J. Sereda, Mechanism of the carbonatation shrinkage of lime and hydrated cement, J. Appl. Chem. 18 (2007) 111–117, https://doi.org/10.1002/jctb.5010180404.
[60] S. Diamond, The microstructure of cement paste and concrete - a visual primer, Cement Concr. Compos. 26 (2004) 919–933, https://doi.org/10.1016/j.cemconcomp.2004.02.028.
[61] M.J. Purton, Comparison of the binding properties of hydrated lime and cement in brick manufacture, J. Appl. Chem. 20 (1970) 293–299, https://doi.org/10.1002/jctb.5010200907.